Advanced Study of Switchable Spin Crossover Compounds

Gavin Craig

ADVANCED STUDY OF SWITCHABLE SPIN CROSSOVER COMPOUNDS

Universitat de Barcelona

Facultat de Química

Departament de Química Inorgànica

Programa de Doctorat: Química Inorgànica Molecular

Grup de Magnetisme i Molècules Funcionals

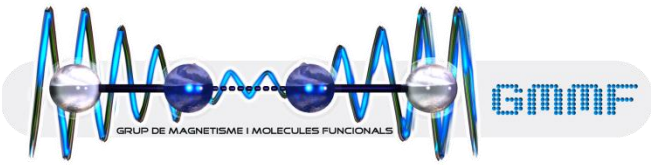

Gavin Craig

Director: Dr. Guillem Aromí Bedmar, Departament de Química Inorgànica

Tutor: Dr. Santiago Alvarez Reverter, Departament de Química Inorgànica

Contents

Chapter 7: Magneto-structural properties of $[Fe(H_4L)_2](ClO_4)_2 \cdot 2THF \cdot H_2O$: The effect of ageing

7.0 Introduction

Although recent advances in the field of SCO have involved the creation of nanowire thermometers,[1-3] the synthesis of bi-stable nanoparticles,[4-7] and the charge-triggered SCO of a polypyridyl Fe(II) system bound between Au electrodes,[8] these increasingly *physical* studies are still founded on *synthetic* chemistry, and its ability to generate new compounds of interest. On this level, there is an ever-greater appreciation of how synthetic parameters such as the solvent employed in the synthesis,[9-12] or the anion used to balance the charge,[13-16] can modify how an Fe(II) ion switches between the two possible spin states, or may even cause the system to remain in the HS state (cf. Chapter 6).

This awareness has even extended to sample preparation, the effects of which may be as fundamental to the magnetic behaviour as the ligand coordinated to the metal centre. This influence is particularly pronounced in the magnetic properties of $[Fe(bapbpy)(NCS)_2]$,[17] where three distinct χT vs. T curves could be obtained from three differently prepared samples of the compound.[18] Each type of preparation was associated with modified degrees of cooperativity in the system, reflected by varying hysteresis widths and levels of the transition's completeness. Within the 3-bpp class of compounds, the delicate balance between the preparative method undertaken, its consequences for the hydration of the system, and resulting variation of the cooperativity and SCO, were the focus of an in-depth study by Marcén *et al.*[19] For example, while the compound $[Fe(3\text{-}bpp)_2](BF_4)_2 \cdot 3H_2O$ displays no appreciable hysteresis in the magnetic measurements, the anhydrous sample has a bi-stable regime measuring 16 K.

In this Chapter, the influence of "ageing" on the compound $[Fe(H_4L)_2](ClO_4)_2 \cdot 2THF \cdot H_2O$ (**7**) is described. On the one hand, the characterisation of the complex was complicated by the sensitivity of the crystals to environmental factors, whilst on the other, this same sensitivity brought about the depth of magnetic behaviour encountered.

7.1 Synthesis

The sensitivity of the magnetic properties of Fe(II) complexes containing the ligand H_4L to the precise synthetic parameters employed has been demonstrated in Chapters 4 and 6, and interpreted in terms of the structural role played by the anions and solvents associated with the cation. Again, two molar equivalents of H_4L were reacted with one mole of $Fe(ClO_4)_2 \cdot H_2O$ with ascorbic acid acting to prevent the oxidation of the Fe(II) ions to Fe(III). The reaction was performed at room temperature in THF, however large orange crystals were obtained by leaving the reaction filtrate to slowly evaporate in the refrigerator, at a temperature of 4°C. Allowing the vessel to reach room temperature, or removal of the crystals from the solvent medium caused an immediate, visible loss of the sample's crystallinity. In spite of this degradation, it was possible to obtain the crystal structure via single crystal X-ray diffraction by quickly removing the sample from the mother liquor and coating it in Paratone oil. The molecular composition of the system was thus shown to be $[Fe(H_4L)_2](ClO_4)_2 \cdot 2THF \cdot H_2O$ (**7**). The elemental analysis of **7** suggests that the observed loss of crystallinity is associated with a partial loss of solvent from the crystal lattice and absorption of moisture from the air, with an important effect on the measured magnetic properties.

7.2 Single crystal X-ray diffraction study

Compound **7** crystallises in the triclinic space group $P\bar{1}$ (Table 7.1), where the asymmetric unit consists of one $[Fe(H_4L)_2]^{2+}$ cation and two ClO_4^- anions which compensate the charge, two lattice molecules of THF, and one of H_2O. As with the other compounds of this series, the H_4L ligands are bound to the Fe(II) ion through their three central N-atoms, resulting in a pseudo-octahedral geometry around the metal centre, and the two ligands display differing conformations of the distal phenol rings with respect to the central coordination pocket; *syn,syn* and *syn,anti* (Figure 7.1). The average Fe-N bond length at 250 K/90 K is 2.156/2.143 Å, which is consistent with a fully HS system at 250 K, and with a partial SCO on lowering the temperature.[20] This very incomplete SCO is also reflected in the parameters θ, Φ, Σ, and Θ,[21-24] which all show relatively minor decreases in their respective values when comparing the high and low temperature structures. The dihedral angle θ formed by the ligands lying in two different planes measures 77.25°/75.07°, while the N3-Fe-N8 angle Φ is 177.09°/176.76°. The parameters Σ and Θ, which are a measure of the extent to which the coordination sphere is distorted

away from an ideal octahedron towards a trigonal prism, are 142.65°/142.45° and 467.17°/460.18°, and these values lie in the range expected for majority high spin systems.[25]

T/K	**250(2)**	**90(2)**
crystal system	Triclinic	Triclinic
space group	P-1	P-1
a/Å	12.467(2)	12.253(3)
b/Å	13.603(3)	13.544(3)
c/Å	17.727(5)	17.523(6)
α/°	105.71(1)	104.07(1)
β/°	102.24(1)	101.46(1)
γ/°	103.78(1)	105.52(1)
V/Å^3	2685.0(11)	2607.6(12)
μ/mm^{-1}	0.577	0.594
Reflections collected	6278	6094
R1 (all data)	0.0625	0.0761
wR2 (all)	0.1939	0.2293
S	1.01	1.02
av. Fe-N/Å	2.156	2.143
octahedral volume/Å^3	12.332	12.123
Σ/°	142.65	142.45
Φ/°	177.09(2)	176.76(2)
θ/°	77.25	75.07
Θ/°	467.17	460.18

Table 7.1: Crystallographic data and selected structural parameters for compound **7**.

The outreaching wings of the aromatic ligand interact through $\pi\cdots\pi$ overlaps and complementary C-H$\cdots\pi$ contacts (averaging 3.619 Å in distance) to induce the 2D "terpyridine embrace" packing arrangement.[26-28] In **7**, the $\pi\cdots\pi$ interactions range in distance from 3.600 to 4.776 Å (see Figure 7.2 and the accompanying table).

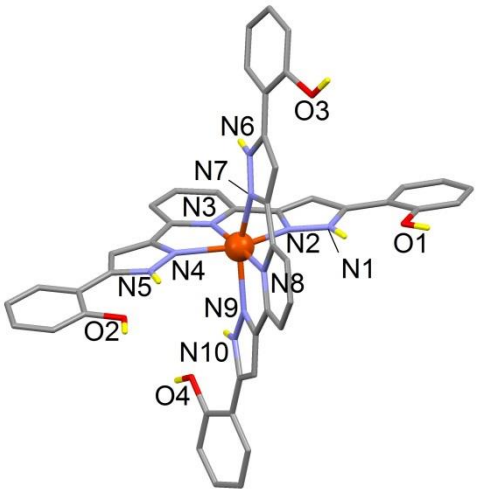

	Bond length/Å	
Bond	250 K	90 K
Fe-N3	2.119(7)	2.109(8)
Fe-N8	2.132(6)	2.119(7)
Fe-N2	2.185(7)	2.156(8)
Fe-N4	2.157(6)	2.148(8)
Fe-N7	2.170(6)	2.159(8)
Fe-N9	2.173(7)	2.167(8)
Average	2.156	2.143

Figure 7.1 and Table 7.2: A Mercury view of the $[Fe(H_4L)_2]^{2+}$ cations in **7**. The hydrogen atoms are omitted for clarity, except those bonded to heteroatoms, shown in yellow. The six Fe-N bond lengths at 250 and 90 K are detailed in the table.

These layers then stack together, bound by the interaction of the ligand's various functional groups with other entities in the lattice such as the water molecules and perchlorate anions. These contacts also bring the pyridyl rings of adjacent cations into a proximity propitious for face-to-face $\pi\cdots\pi$ stacking. The pyrazolyl rings participate in hydrogen bonding interactions with the oxygen atoms of the nearby perchlorate anions, with an average distance of 2.936/2.896 Å (Figure 7.3). The perchlorate anions then link to the phenol group of a cation in an adjacent layer, with an average strength of 2.854/2.786 Å. These interactions are of the same order of magnitude as those previously observed in systems of this type. The average interlayer distance between Fe(II) atoms measures 9.699/9.645 Å.

In these crystal packing arrangements, the presence of hydrogen bonding through one of the pyrazolyl rings in an H_4L ligand precludes the possibility of the other pyrazolyl ring establishing such interactions, and as a result supramolecular contacts are conducted through the external phenol ring. In **7**, however, there is an arrangement which allows for the usual pattern of interactions, and also permits the binding of a water molecule to the normally unemployed pyrazolyl ring (N9-H9A$\cdots$O1W = 2.994/2.977 Å) (Figure 7.3, right). It is unclear whether the effect of the water molecule on the electron density within the pyrazolyl ring favours the triplet or singlet state of the Fe(II) centre, as both possibilities have been discussed previously.[30-32]

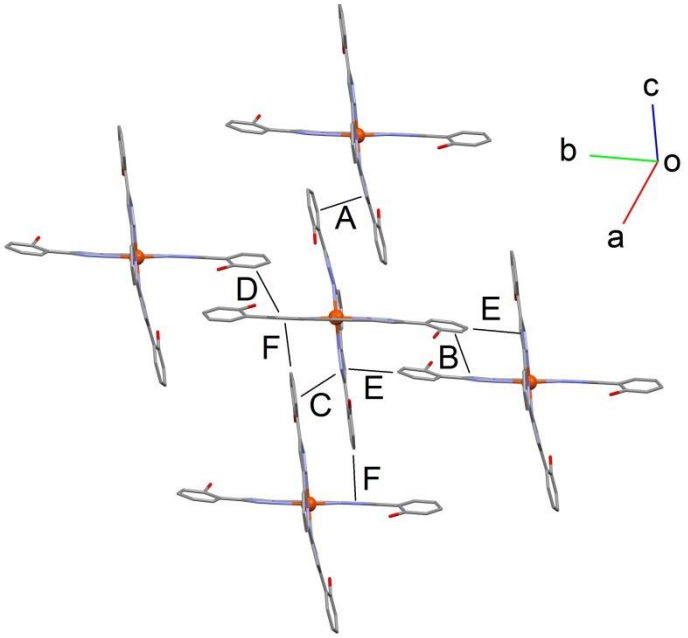

Contact	Labels	Distance/Å	
π*···*π		250 K	90 K
A	pz···phen	3.600(5)	3.504(6)
B	pz···phen	4.776(5)	4.858(6)
C	pz···phen	4.486(5)	4.396(6)
D	pz···phen	4.416(5)	4.375(6)
C-H···*π*			
E	C26-H26A···pz	3.685(11)	3.709(13)
F	C3-H3A···pz	3.553(11)	3.511(12)

Figure 7.2 and Table 7.3: A representation of the 2D networks formed in **7**, induced by *π*···*π* and C-H···*π* interactions. The hydrogen atoms are omitted for clarity. The table details the distances for each contact at 250 and 90 K, while pz = pyrazolyl ring and phen = phenol ring.

7.3 Magnetic properties

The magnetic properties of a sample of **7** that had been freshly removed from the mother liquor were measured in the 5-300 K temperature range under a magnetic field of 5 kG, and are shown in Figure 7.4. The fresh samples display a value of the molar magnetic susceptibility product χT of 3.1 $cm^3mol^{-1}K$ at 300 K, in agreement with the expected value for an Fe(II) ion in the HS state ($S = 2$, $\chi T = 3.0$ $cm^3mol^{-1}K$ for $g = 2$),[33] and also consistent with the crystal structure described above. On lowering the temperature at 1 $Kmin^{-1}$, this value is maintained until around 140 K, where a partial SCO occurs,

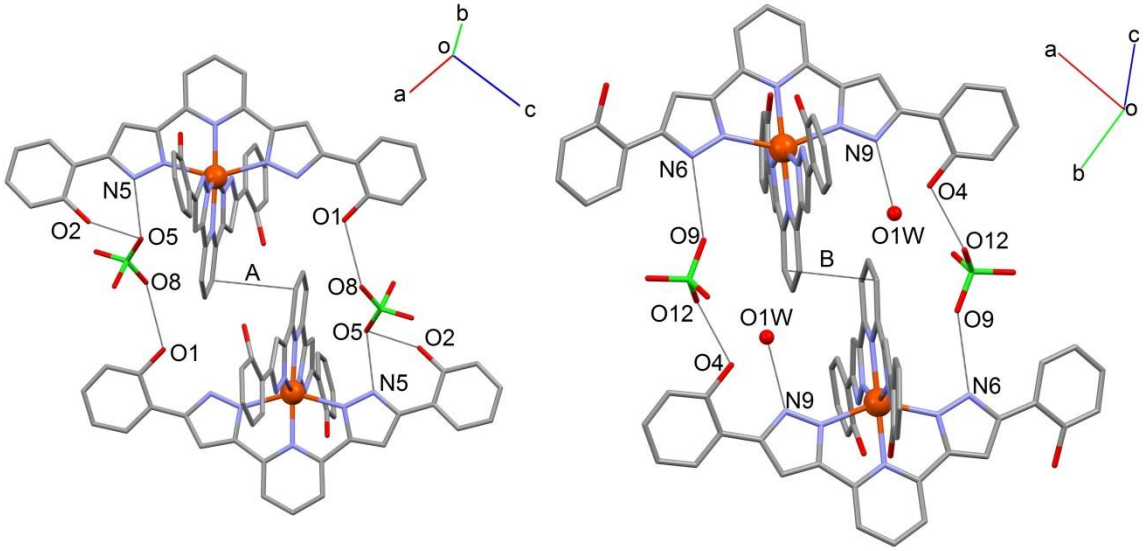

Contact	Distance/Å	
(left)	250 K	90 K
N5-H5···O5	2.946(9)	2.908(11)
O1-H1···O8	2.931(18)	2.566(17)
O2-H2···O5	3.039(9)	2.984(18)
A = py···py	4.550(5)	4.447(6)
Fe···Fe	9.559(3)	9.549(2)
(right)		
N6-H6···O9	2.925(9)	2.884(11)
N9-H9···O1W	2.994(11)	2.977(12)
O4-H4···O12	2.776(13)	2.807(11)
B = py···py	4.670(4)	4.716(5)
Fe···Fe	9.839(2)	9.740(3)

Figure 7.3 and Table 7.4: The hydrogen bonding motifs and metric parameters for the interactions that exist between the 2D layers in **7**, with hydrogen atoms omitted for clarity.

leading to a value of χT = 2.5 $cm^3mol^{-1}K$ below 80 K. At the lowest temperatures measured there is a decrease in the magnetic response due to zero field splitting effects.[34] Raising the temperature at the same rate retraces the curve obtained in the cooling mode, until the divergence of χT at 80 K. The transition to the HS state begins at 90 K, and the hysteresis loop measures 8 K.

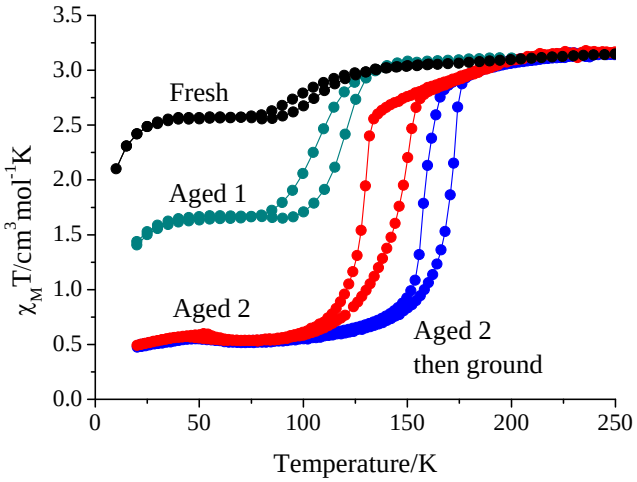

Figure 7.4: The molar magnetic susceptibility product, χT *vs*. the temperature, T, for various samples of **7**, as labelled in the figure.

As discussed in Section 7.1, exposure of the crystal samples of **7** to air results in a visible degradation of the crystal quality, a process attributed to the possible interchange of atmospheric water for solvent molecules within the crystal lattice. This "ageing", which occurs over a period of several months once the sample is removed from the solvent, has a subsequent effect on the magnetic properties presented by the system (Figure 7.4). In common with the fresh samples, the aged compound shows a hysteresis loop of χT on performing a thermal cycle. However, spin transitions recorded for aged compounds are observed to be more complete in nature, with lower residual HS populations at low temperatures (χT values ranging from 1.65 to 0.55 cm^{3}mol^{-1}K), and are associated with broader bi-stable domains, achieving a maximum hysteresis width of 21 K for the fully aged sample. This broadening is concomitant with a displacement of the thermal SCO to higher temperatures which, for the latter case, give rise to values of $T_{1/2}(\downarrow)$ = 129 K and $T_{1/2}(\uparrow)$ = 150 K.

The impact that grinding a crystal sample may have on the system's magnetic properties was demonstrated in Chapter 4, where milling the polycrystalline form of compound **1** led to a powder sample devoid of SCO behaviour. In the case of fresh crystals of **7**, reducing the particle size has no effect on the SCO properties, and the same partial transition with hysteresis is observed. This contrasts with the change observed in the χT vs. T curve recorded after grinding the fully aged sample of **7**. While the HS and LS fractions corresponding to high and low temperature are maintained with respect to the non-ground fully aged sample, the precise nature of the transition is modified – shifted to higher

temperatures still ($T_{1/2}(\downarrow)$ = 162 K and $T_{1/2}(\uparrow)$ = 172 K), and associated with a more abrupt conversion between the quintet and singlet states.

The magnetic measurements described serve to highlight the extent to which SCO behaviour can depend on subtle changes in chemical composition beyond the spin active units, and their sensitivity to environmental conditions.

7.4 Differential Scanning Calorimetry

The energetics of the transitions observed for the aged and ground sample of **7** were investigated with differential scanning calorimetry in both the heating and cooling modes. Figure 7.5 shows the excess heat capacity, ΔC_P, associated with the cooling mode derived by subtracting a normal heat capacity curve from the heat capacity measurement, and following Equation 1.4 to deduce ΔS = 21.9 $Jmol^{-1}K^{-1}$ and ΔH = 3.13 $kJmol^{-1}$, for the HS→LS transition.[35] The value of the excess entropy lies above that expected for a change purely of the spin state ($R\ln(5)$ = 13.4 $Jmol^{-1}K^{-1}$), although it is relatively low, which may be ascribed to the incomplete nature of the SCO or the poor crystallinity of the sample. The maxima of the curve lies at 144 K, which is below that seen in the magnetic measurements, an effect which is attributed to the different cooling rate used in the DSC measurements (10 $Kmin^{-1}$) compared to that used in the SQUID (1 $Kmin^{-1}$).

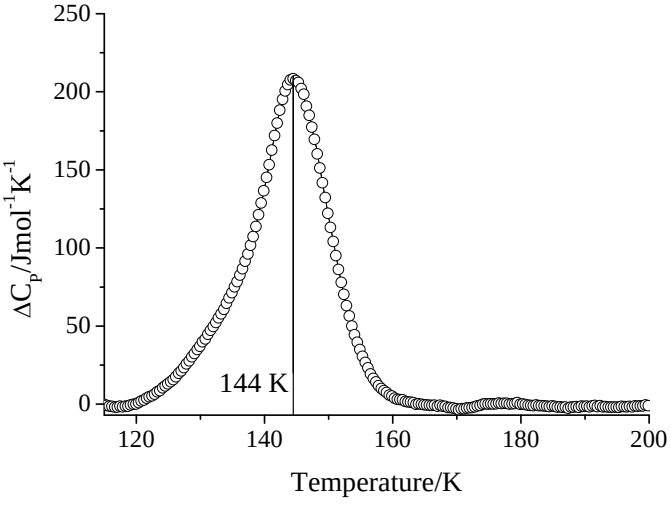

Figure 7.5: The excess heat capacity, ΔC_P, *vs*. *T* for compound **7**.

7.5 Concluding remarks

The compound $[Fe(H_4L)_2](ClO_4)_2 \cdot 2THF \cdot H_2O$ (**7**) is a further demonstration of the diversity of SCO behaviour to be found in the family of mononuclear Fe(II) systems

based on the ligand H_4L. The study of this compound has also highlighted the degree to which the ability of a complex to switch between the two possible spin states, and the cooperativity associated with this process, depends on a factor such as the hydration of the sample measured. This dependence was deduced from the observation that, with the passage of time, the spin transition in **7** became more complete and increasingly cooperative.

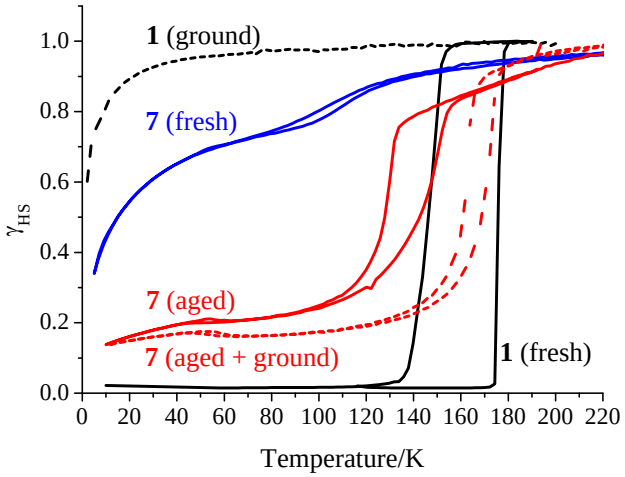

Figure 7.6: The molar magnetic susceptibility product, χT *vs*. the temperature, *T*, for compounds **1** and **7**, in different states of preparation (labelled). Ground samples are shown with dotted lines, fresh samples with solid lines.

This compound displayed a further level of complexity, in that the SCO behaviour is related to the particle size as well as the degree of ageing of the sample (Figure 7.6). Thus, while grinding the fresh crystal sample, reducing the particle size, has no effect on the nature of the spin transition, carrying out the same procedure on the fully aged system leads to a more cooperative SCO at higher temperatures, and modifies the hysteresis width. This runs contrary to the expectation that grinding would induce defects in the lattice, impacting upon the intermolecular interactions between the cations, and lead to a diminished spin transition.[36] Such was the case of compound **1**, where a reduction of particle size caused the disappearance of the 40 K hysteresis loop and the SCO of the $[Fe(H_4L)_2]^{2+}$ cations, and yielded a HS system over the full temperature range measured. Therefore, compounds **1** and **7** underline the importance of sample preparation in SCO research, which is shown to not only depend on chemical factors, but also on mechanical effects.

7.6 References

1. C. M. Quintero, I. y. A. Gural'skiy, L. Salmon, G. Molnar, C. Bergaud and A. Bousseksou, *J. Mater. Chem.*, 2012, **22**, 3745-3751.
2. A. Bousseksou, G. Molnar, L. Salmon and W. Nicolazzi, *Chem. Soc. Rev.*, 2011, **40**, 3313-3335.
3. L. Salmon, G. Molnar, D. Zitouni, C. Quintero, C. Bergaud, J.-C. Micheau and A. Bousseksou, *J. Mater. Chem.*, 2010, **20**, 5499-5503.
4. S. Pillet, P. Durand, E.-E. Bendeif, C. Carteret, M. Bouazaoui, H. El Hamzaoui, B. Capoen, L. Salmon, S. Hebert, J. Ghanbaja, L. Aranda and D. Schaniel, *J. Mater. Chem. C*, 2013, 10.1039/C1033TC00546A.
5. J. R. Galán-Mascarós, E. Coronado, A. Forment-Aliaga, M. Monrabal-Capilla, E. Pinilla-Cienfuegos and M. Ceolin, *Inorg. Chem.*, 2010, **49**, 5706-5714.
6. T. Forestier, A. Kaiba, S. Pechev, D. Denux, P. Guionneau, C. Etrillard, N. Daro, E. Freysz and J.-F. Letard, *Chem.-Eur. J.*, 2009, **15**, 6122-6130.
7. E. Coronado, J. R. Galán-Mascarós, M. Monrabal-Capilla, J. Garcia-Martinez and P. Pardo-Ibañez, *Adv. Mat.*, 2007, **19**, 1359-1360.
8. V. Meded, A. Bagrets, K. Fink, R. Chandrasekar, M. Ruben, F. Evers, A. Bernand-Mantel, J. S. Seldenthuis, A. Beukman and H. S. J. van der Zant, *Phys. Rev. B*, 2011, **83**, 245415.
9. R.-J. Wei, J. Tao, R.-B. Huang and L.-S. Zheng, *Inorg. Chem.*, 2011, **50**, 8553-8564.
10. B. Li, R. J. Wei, J. Tao, R. B. Huang, L. S. Zheng and Z. P. Zheng, *J. Am. Chem. Soc.*, 2010, **132**, 1558-1566.
11. E. Coronado, J. C. Dias, M. C. Giménez-López, C. Giménez-Saiz and C. J. Gómez-Garcia, *J. Mol. Struct.*, 2008, **890**, 215-220.
12. W. Zhang, F. Zhao, T. Liu, M. Yuan, Z.-M. Wang and S. Gao, *Inorg. Chem.*, 2007, **46**, 2541-2555.
13. I. Nemec, R. Herchel, R. Boca, Z. Travnicek, I. Svoboda, H. Fuess and W. Linert, *Dalton Trans.*, 2011, **202**, 2020.
14. J. A. Kitchen, N. G. White, G. N. L. Jameson, J. L. Tallon and S. Brooker, *Inorg. Chem.*, 2011, **50**, 4586-4597.
15. X. Bao, J. D. Leng, Z. S. Meng, Z. J. Lin, M. L. Tong, M. Nihei and H. Oshio, *Chem.-Eur. J.*, 2010, **16**, 6169-6174.
16. M. M. DiÌ‚rtu, A. Rotaru, D. Gillard, J. Linares, E. Codjovi, B. Tinant and Y. Garcia, *Inorg. Chem.*, 2009, **48**, 7838-7852.
17. S. Bonnet, M. A. Siegler, J. S. Costa, G. Molnár, A. Bousseksou, A. L. Spek, P. Gamez and J. Reedijk, *Chem. Commun.*, 2008, 5619-5621.
18. S. Bonnet, G. Molnár, J. S. Costa, M. A. Siegler, A. L. Spek, A. Bousseksou, W. T. Fu, P. Gamez and J. Reedijk, *Chem. Mat.*, 2009, **21**, 1123-1136.
19. S. Marcén, L. Lecren, L. Capes, H. A. Goodwin and J.-F. Létard, *Chem. Phys. Lett.*, 2002, **358**, 87-95.
20. A. Hauser, *Top. Curr. Chem.*, 2004, **233**, 49-58.
21. P. Guionneau, M. Marchivie, G. Bravic, J.-F. Létard and D. Chasseau, *Top. Curr. Chem.*, 2004, **234**, 97-128.
22. J. M. Holland, J. A. McAllister, C. A. Kilner, M. Thornton-Pett, A. J. Bridgeman and M. A. Halcrow, *J. Chem. Soc. Dalton Trans.*, 2002, 548-554.
23. J. K. McCusker, A. L. Rheingold and D. N. Hendrickson, *Inorg. Chem.*, 1996, **35**, 2100-2112.

24. M. G. B. Drew, C. J. Harding, V. McKee, G. G. Morgan and J. Nelson, *J. Chem. Soc., Chem. Commun.*, 1995, 1035-1038.
25. M. A. Halcrow, *Chem. Soc. Rev.*, 2011, **40**, 4119-4142.
26. M. L. Scudder, D. C. Craig and H. A. Goodwin, *CrystEngComm*, 2005, **7**, 642-649.
27. K. H. Sugiyarto, W. A. McHale, D. C. Craig, A. D. Rae, M. L. Scudder and H. A. Goodwin, *Dalton Trans.*, 2003, 2443-2448.
28. M. L. Scudder, H. A. Goodwin and I. G. Dance, *New J. Chem.*, 1999, **23**, 695-705.
29. A. L. Spek, *J. App. Cryst.*, 2003, **36**, 7-13.
30. T. D. Roberts, F. Tuna, T. L. Malkin, C. A. Kilner and M. A. Halcrow, *Chem. Sci.*, 2012, **3**, 349-354.
31. S. A. Barrett, C. A. Kilner and M. A. Halcrow, *Dalton Trans.*, 2011, 12021-12024.
32. K. H. Sugiyarto, K. Weitzner, D. C. Craig and H. A. Goodwin, *Aust. J. Chem.*, 1997, **50**, 869-873.
33. O. Kahn, *Molecular Magnetism, Wiley VCH*, 1993.
34. M. A. Halcrow, *Chem. Soc. Rev.*, 2008, **37**, 278-289.
35. M. Sorai, Y. Nakazawa, M. Nakano and Y. Miyazaki, *Chem. Rev.*, 2013, **113**, 41-122.
36. P. Gütlich, A. Hauser and H. Spiering, *Angew. Chem. Int. Ed.*, 1994, **33**, 2024-2054.